CRYSTAL GROWTH & DESIGN

Article

pubs.acs.org/crystal

Micropillar Cavity Containing a CdTe Quantum Dot with a Single Manganese Ion

W. Pacuski,*[,†,‡] T. Jakubczyk,[†,‡] C. Kruse,[†,⊥] J. Kobak,[‡] T. Kazimierczuk,[‡] M. Goryca,[‡] A. Golnik,[‡] P. Kossacki,[‡] M. Wiater,[§] P. Wojnar,[§] G. Karczewski,[§] T. Wojtowicz,[§] and D. Hommel[†]

[†]Institute of Solid State Physics, University of Bremen, PO Box 330 440, D-28334 Bremen, Germany

[‡]Institute of Experimental Physics, Faculty of Physics, University of Warsaw, Hoża 69, PL-00-681 Warsaw, Poland

[§]Institute of Physics, Polish Academy of Sciences, al. Lotników 32/46, PL-02-668 Warsaw, Poland

ABSTRACT: We report on the method of fabrication of a photonic microstructure that contains a single magnetic ion. Exactly one manganese ion was introduced into a self-assembled CdTe quantum dot, which was located in a ZnTe based micropillar cavity. The multistep fabrication procedure includes molecular beam epitaxy growth, optical characterization, and focused ion beam etching. Realization of the structure was confirmed by the observation of spectroscopic exciton lines split by six due to the exchange interaction with a manganese ion. The cavity mode was tuned to the quantum dot emission energy by a variation of the temperature. The presented technology is developed to be applied in optoelectronics based on solitary dopants.

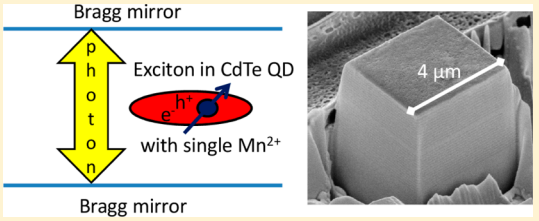

INTRODUCTION

A quantum dot (QD) with a single magnetic ion is an example of a simple but very interesting quantum system where the exciton interacts with a single localized spin,[1−3] which is long-lived and more robust than the spin of carriers.[4−6] Recent reports[7−10] show a possibility of efficient control of the spin state in such a system. Placing a QD with a Mn^{2+} ion in a photonic environment opens new perspectives[11,12] for optical manipulation of quantum states and for new applications in the information technologies, in particular in solotronics[13,14] (solitary dopant optoelectronics). Utilization of photonic structures, such as a planar microcavity[15,16] or a micropillar,[17−20] has many potential advantages such as improvement of the photon extraction efficiency,[21] localized spin read-out with only weak perturbation, and enhancement of the coupling of a QD exciton to light possessing selected properties[22,23] (wavelength and propagation direction). Furthermore, the creation of a mixed quantum state of a photon and a localized magnetic moment in the strong coupling regime and photon mediated spin−spin coupling for spintronics or quantum computing might be possible.[12,13]

In this work, we present the first successful incorporation of self-assembled QDs with single Mn^{2+} ions into a planar ZnTe cavity and the subsequent spatial and spectral matching of a pillar cavity eigenmode to a quantum dot exciton coupled to a single Mn^{2+} ion. Compared with nanocrystal QDs,[24−33] using single self-assembled QDs in this work results in very sharp excitonic photoluminescence (PL) lines, which allow us to observe spin splitting related to the interaction of the quantum dot exciton with a single magnetic dopant.

EPITAXY

The crystal was grown by using a three-step approach employing alternately two different molecular beam epitaxy (MBE) chambers for the deposition of the distributed Bragg reflectors and the quantum dots, respectively. The bottom and the top part of the structure was grown at the University of Bremen, while the middle part containing magnetic QDs was grown in the Institute of Physics in Warsaw, where the necessary Mn source was available.

The design of the structure is presented in Figure 1a. The growth was performed on a GaAs:Si(001) substrate. First, a thin ZnSe layer, which is almost lattice matched to GaAs, has been deposited to initiate a good growth start. The next layer is a thick ZnTe buffer, which has a significantly larger lattice parameter than ZnSe or GaAs. Therefore, the ZnTe layer relaxes during growth, and after a thickness of about 1 μm, it exhibits a lattice parameter that is very close to that of unstrained ZnTe. Next, there is a bottom distributed Bragg reflector, which contains 14.5 pairs of alternating layers with high and low refractive index. The high refractive index layer is made of ZnTe, and the layer with the low refractive index consists of a short period ZnTe/MgSe/ZnTe/MgTe superlattice.[34]

After deposition of the first DBR, the lower part of the ZnTe microcavity (54 nm) was grown and a reflectivity spectrum was measured [Figure 1b, spectrum 1]. This spectrum shows a stopband typical for a DBR, which is centered at an energy of about 1900 meV, close to the typical emission energy of CdTe/

Received: September 15, 2013
Revised: December 31, 2013
Published: February 7, 2014

   dx.doi.org/10.1021/cg4013763 | *Cryst. Growth Des.* 2014, 14, 988−992

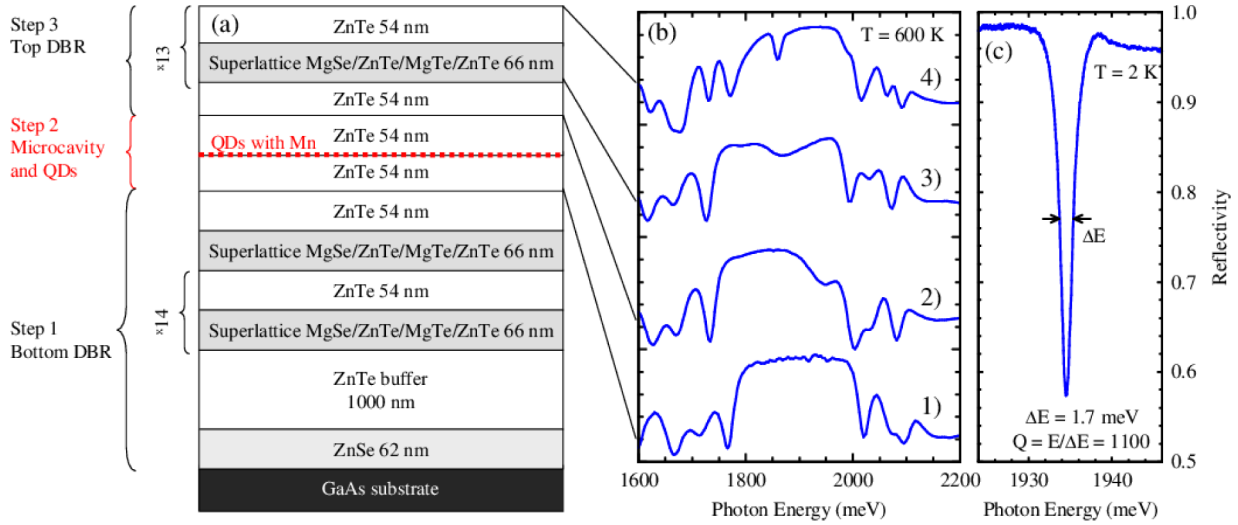

Figure 1. (a) Scheme of layers grown using molecular beam epitaxy. (b) In situ reflectivity spectra measured after various growth steps. From bottom to the top, (1) after growth of the bottom DBR, (2) after growth of the cavity and QDs, (3) after completing the cavity, and (4) at the end of the growth. (c) Low temperature reflectivity measured with a spot of about 2 μm diameter. The full width at half minimum of the cavity mode is 1.7 meV, which corresponds to a quality factor, Q = 1100, of the cavity.

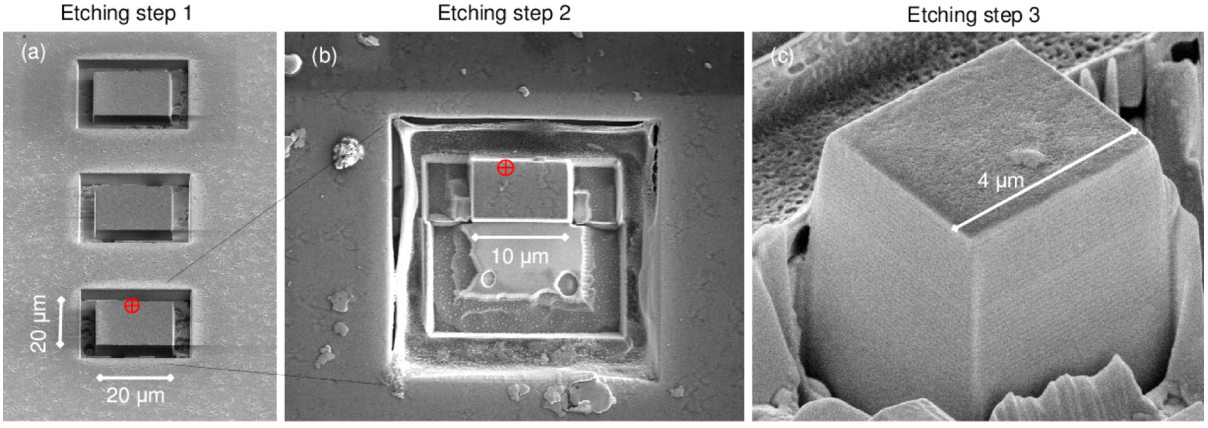

Figure 2. Three step etching using a focused ion beam (FIB). (a) Step 1, square mesas of sufficient size (20 μm by 20 μm) to ensure reasonable probability of finding a QD with a single Mn^{2+} ion inside. PL measurements revealed that the bottom mesa contains such a QD (marked by red circle). (b) Step 2, smaller (10 μm by 5 μm) mesa cut out of larger mesa, still contains a QD with a single Mn ion. (c) Step 3, square micropillar with a QD containing exactly one Mn ion. All photographs were realized using scanning electron microscopy.

ZnTe quantum dots.[35,36] At this point, the growth was interrupted and the sample was cooled and covered by a thick layer of amorphous tellurium in order to protect the epitaxial layers before exposing them to air. Next, the sample was taken out from the first MBE and transported to the other epitaxy facility (Institute of Physics, Warsaw) in order to grow the magnetic quantum dots.[4,37] After introduction of the sample to the MBE machine, the amorphous tellurium was removed by heating the sample to the ZnTe growth temperature and the next 54 nm of ZnTe was deposited. At this point, in the middle of the incomplete cavity, a very thin layer (about 6 ML) of CdTe with a small amount of Mn was deposited.[9,36] In order to transform this layer into quantum dots,[35] the sample was cooled and its surface was covered by tellurium. In the next step, the sample was heated again to the ZnTe growth temperature, and the RHEED diffraction pattern revealed a transformation of the surface from two-dimensional (streaky pattern) to three-dimensional (spotty pattern), which is an expected signature of the quantum dot formation. The QDs were covered by a cap layer of about 50 nm of ZnTe. Then sample was cooled to room temperature and covered by a thick layer of amorphous tellurium again for surface protection during the sample transfer back to the MBE laboratory at the University of Bremen.

In the final step, the sample was introduced into the ultrahigh vacuum of an MBE chamber once again, and the amorphous tellurium protection layer was evaporated from the surface. At this stage, the determination of the actual thickness of the cavity was crucial for the successful continuation of the MBE growth with respect to the correct optical thickness of the cavity. The reflectivity measurement [Figure 1b, spectrum 2] shows that the spectral position of the optical cavity mode is on the high energy side of the stopband, what indicates that the cavity was not completed yet, as intended (i.e., cavity thickness below λ/n). When the growth of ZnTe was started again, the mode moved toward low energy with increasing cavity thickness and reached the central position of the stopband [Figure 1b, spectrum 3]. This indicated that the cavity reached the correct thickness and the growth of the top DBR could have been

dx.doi.org/10.1021/cg4013763 | Cryst. Growth Des. 2014, 14, 988−992

started. The top DBR contains 13 pairs of layers with high and low refractive index.

After completing the whole vertical resonator structure, the optical cavity mode [Figure 1b, spectrum 4] was sharp and only slightly shifted from the intended spectral position in the middle of the stopband. Measurements at helium temperature with high spectral and spatial resolution revealed a very sharp optical mode in the reflectivity spectrum [Figure 1c]. Its fwhm is equal to 1.7 meV, which corresponds to a quality factor of 1100. The spectral position of the cavity mode is close to intended 1900 meV, where the probability of finding a well isolated QD with a single Mn^{2+} ion is significant.[9] In fact, several QDs with characteristic single Mn^{2+} sextuplets[1,38] were observed in micro-PL spectra of our sample.

ETCHING MICROSTRUCTURES AND PL MONITORING

Due to low density of QDs containing exactly one Mn^{2+} ion, a focused ion beam (FIB) etching was employed to provide a reference for positioning such QDs on the sample. We etched several square mesas with 20 μm side length [Figure 2a]. A QD with a single Mn^{2+} ion was found in the photoluminescence spectrum of one of the mesas [Figure 3b]. The spectrum of

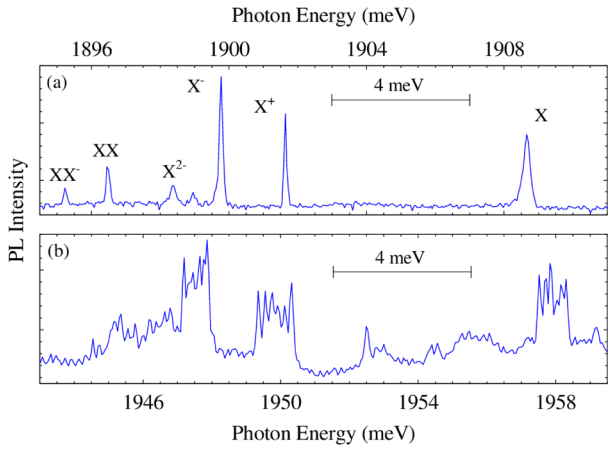

Figure 3. Photoluminescence spectra of individual quantum dots at helium temperatures. (a) PL spectrum of a typical CdTe quantum dot with unambiguously identified transitions. (b) PL spectrum of the CdTe quantum dot that contains a single Mn^{2+} ion, measured after the third etching step, that is, on the structure shown in Figure 2c. Comparing spectra of a typical QD without Mn^{2+} and the one with a single Mn^{2+} ion, the separation energies of various exciton lines are in fact very similar, but each exciton transition in the magnetic dot is split due to interaction with the Mn^{2+} ion. For the neutral exiton (X) line, a 6-fold splitting is expected and indeed observed. For charged excitons (X^+ and X^-) and higher complexes like X^{2-}, and XX^- more complex spectra are expected[7] but are difficult to resolve in detail in the PL of the presented magnetic dot.

such QD is very similar to spectra of typical QDs without manganese ions [Figure 3a]. It consist of a neutral (X) and charged (X^+ and X^-) exciton lines and lines related to other exciton complexes such as X^{2-} and XX. The difference between QD with and without a single Mn^{2+} ion inside is 6-fold splitting of the excitonic line in theh QD with Mn^{2+} ion.[1] This is due to the s,p−d exchange interaction and six projections of 5/2 spin of Mn^{2+} (+5/2, +3/2, +1/2, −1/2, −3/2, −5/2). During the accumulation time of the PL spectrum, the Mn^{2+} ion occupies every particular spin state many times while the emission energy of the exciton depends on the relative spin projection of the Mn^{2+} ion and the exciton.

Using the sides of the square as coordinate axes, we determined the exact position of the suitable QD. This allows us to etch a smaller mesa (5 μm by 10 μm, Figure 2b) containing this QD. It should be noted that the emission properties of the QD were not affected by the FIB milling according to the PL measurements. Once more the position of the QD with a single Mn^{2+} ion was determined and a third FIB etching step was performed in order to realize the 4 μm pillar around that specific QD [Figure 2c]. A final check by PL confirmed that the QD with the single Mn^{2+} ion is still present and emits the characteristic 6-fold split lines.

SPECTRAL TUNING TO THE RESONANCE OF THE QD AND MICROCAVITY

The reflectivity measurement of the 4 μm pillar is shown in Figure 4b. Cavity mode is much broader than measured for the optimal place in the sample, just after growth [Figure 1c]. There could be several reasons for that. Measurement of the micropillar was optimized for collecting PL from a broad range of angles, so reflectivity mode is wider than in the perpendicular reflectivity experiment in Figure 1c. The sample is non-homogeneous, and cavity mode energy and width strongly depends on the point of the sample. Low refractive index layers contain magnesium, so they can be slightly degraded after several months. The part of the sample with the identified QD with single Mn was several times cooled and heated in various cryostats. Finally FIB etching and SEM imaging also induces changes optical properties of micropillars.

Resonant mode energy is about 1942 meV at low temperature [Figure 4b], that is, at a slightly lower energy than the emission of the QD, which is at about 1950 meV. Therefore, it is possible to spectrally tune the QD emission line to the cavity mode using temperature. The QD emission energy depends on energy gap of CdTe and ZnTe, so it decreases with increasing the temperature.

The spectral position of the cavity mode depends on the refractive index of the materials used, which also decreases with temperature but at a much weaker pace. Consequently, at about 70 K the QD line crosses the center of the optical mode [Figure 4a]. Unfortunately, above several tens of kelvins, the QDs' lines become much broader due to phonons, which means that experiments at the resonance with the single sixtuplet cannot be performed for this particular QD with the resonance at 70 K. Also decay time measurements of Purcell effect, as we recently demonstrated[39,40] for a similar structure without Mn, cannot be performed for such high temperature (70 K) because background photoluminescence is stronger than individual QD PL. The optimal resonance temperature is preferably below 10 K. Thus, this work represents a proof of concept for the effective technological procedure of making a photonic microstructure that contains a QD with a single Mn^{2+} ion inside. The procedure can be improved by combining low-temperature FIB milling with low-temperature in situ cathodoluminescence used to precisely determine the position of the QD.

CONCLUSIONS

We realized a photonic pillar microstructure that was intentionally fabricated around a selected CdTe QD with a single Mn^{2+} ion inside by FIB etching. The spatial position of

dx.doi.org/10.1021/cg4013763 | Cryst. Growth Des. 2014, 14, 988−992

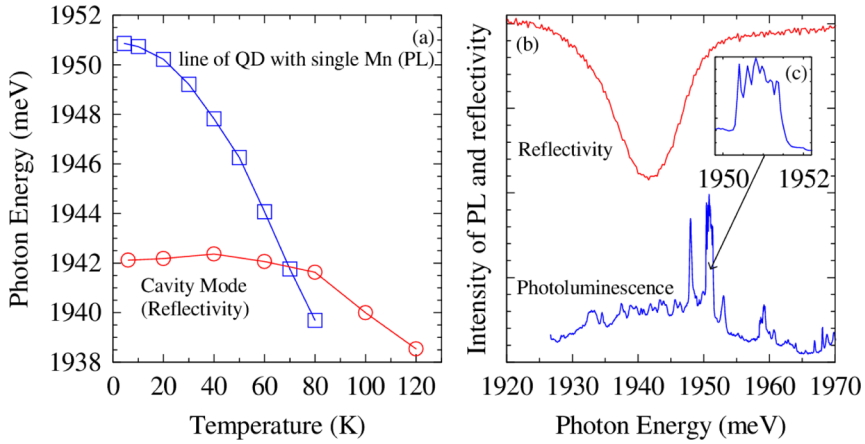

Figure 4. (a) Position of the cavity mode (squares) and line related to the QD with the single Mn^{2+} ion (circles), as a function of temperature. (b) Corresponding reflectivity and PL spectrum measured at about T = 5 K. (c) Magnification of the 6-fold split PL line of the QD with a single Mn^{2+} ion.

the QD was determined via spatially resolved micro-PL. In situ reflectivity monitoring turned out to be a crucial tool to control several successive epitaxial growth steps of a vertical resonator even when the epitaxial deposition is performed in different facilities. The exact matching of the QD emission line to the mode of the micropillar cavity was realized using temperature tuning during the optical experiments. This kind of approach shows the possibility to fabricate demanding cavity structures even if the building blocks can only be realized in different laboratories. The achievement discussed here demonstrates that effects based on a single spin can be combined with cavity quantum electrodynamics.

AUTHOR INFORMATION

Corresponding Author

*E-mail: Wojciech.Pacuski@fuw.edu.pl.

Present Address

⊥Department of Physics, University of Osnabrück, 49076 Osnabrück, Germany.

Notes

The authors declare no competing financial interest.

ACKNOWLEDGMENTS

This work was supported by Alexander von Humboldt Foundation and Polish public funds (NCN projects DEC-2011/01/B/ST3/02406, DEC-2011/02/A/ST3/00131, DEC-2011/01/N/ST3/04536, NCBiR project LIDER, and Foundation for Polish Science). Project was carried out with the use of CePT, CeZaMat, and NLTK infrastructures financed by the European Union, the European Regional Development Fund within the Operational Programme "Innovative economy". The research leading to these results has received funding from the European Union Seventh Framework Programme (FP7/2007-2013) under Grant Agreement No. 316244.

REFERENCES

(1) Besombes, L.; Léger, Y.; Maingault, L.; Ferrand, D.; Mariette, H.; Cibert, J. *Phys. Rev. Lett.* **2004**, *93*, No. 207403.
(2) Kudelski, A.; Lemaître, A.; Miard, A.; Voisin, P.; Graham, T. C. M.; Warburton, R. J.; Krebs, O. *Phys. Rev. Lett.* **2007**, *99*, No. 247209.
(3) Goryca, M.; Plochocka, P.; Kazimierczuk, T.; Wojnar, P.; Karczewski, G.; Gaj, J. A.; Potemski, M.; Kossacki, P. *Phys. Rev. B* **2010**, *82*, No. 165323.
(4) Goryca, M.; Ferrand, D.; Kossacki, P.; Nawrocki, M.; Pacuski, W.; Maélana, W.; Gaj, J. A.; Tatarenko, S.; Cibert, J.; Wojtowicz, T.; Karczewski, G. *Phys. Rev. Lett.* **2009**, *102*, No. 046408.
(5) Le Gall, C.; Brunetti, A.; Boukari, H.; Besombes, L. *Phys. Rev. Lett.* **2011**, *107*, No. 057401.
(6) Ochsenbein, S. T.; Gamelin, D. R. *Nat. Nanotechnol.* **2010**, *6*, 112.
(7) Léger, Y.; Besombes, L.; Fernéndez-Rossier, J.; Maingault, L.; Mariette, H. *Phys. Rev. Lett.* **2006**, *97*, No. 107401.
(8) Gall, C. L.; Besombes, L.; Boukari, H.; Kolodka, R.; Cibert, J.; Mariette, H. *Phys. Rev. Lett.* **2009**, *102*, No. 127402.
(9) Goryca, M.; Kazimierczuk, T.; Nawrocki, M.; Golnik, A.; Gaj, J. A.; Kossacki, P.; Wojnar, P.; Karczewski, G. *Phys. Rev. Lett.* **2009**, *103*, No. 087401.
(10) Le Gall, C.; Brunetti, A.; Boukari, H.; Besombes, L. *Phys. Rev. B* **2012**, *85*, No. 195312.
(11) Andrade, J. A.; Aligia, A. A.; Quinteiro, G. F. *J. Phys.: Condens. Matter* **2011**, *23*, No. 215304.
(12) Andrade, J. A.; Aligia, A. A.; Quinteiro, G. F. *Phys. Rev. B* **2012**, *85*, No. 165421.
(13) Koenraad, P. M.; Flatté, M. E. *Nat. Mater.* **2011**, *10*, 91−100.
(14) Kobak, J.; Smoleński, T.; Goryca, M.; Papaj, M.; Gietka, K.; Bogucki, A.; Koperski, M.; Rousset, J.-G.; Suffczyński, J.; Janik, E.; Nawrocki, M.; Golnik, A.; Kossacki, P.; Pacuski, W. *Nat. Commun.* **2014**, *5*, 3191.
(15) Weisbuch, C.; Nishioka, M.; Ishikawa, A.; Arakawa, Y. *Phys. Rev. Lett.* **1992**, *69*, 3314−3317.
(16) Dang, L. S.; Heger, D.; André, R.; Bœuf, F.; Romestain, R. *Phys. Rev. Lett.* **1998**, *81*, 3920−3923.
(17) Gérard, J. M.; Sermage, B.; Gayral, B.; Legrand, B.; Costard, E.; Thierry-Mieg, V. *Phys. Rev. Lett.* **1998**, *81*, 1110−1113.
(18) Kruse, C.; Ulrich, S. M.; Alexe, G.; Roventa, E.; Kröger, R.; Brendemühl, B.; Michler, P.; Gutowski, J.; Hommel, D. *Phys. Status Solidi B* **2004**, *241*, 731−738.
(19) Kruse, C.; Pacuski, W.; Jakubczyk, T.; Kobak, J.; Gaj, J. A.; Frank, K.; Schowalter, M.; Rosenauer, A.; Florian, M.; Jahnke, F.; Hommel, D. *Nanotechnology* **2011**, *22*, No. 285204.
(20) Ren, Q.; Lu, J.; Tan, H. H.; Wu, S.; Sun, L.; Zhou, W.; Xie, W.; Sun, Z.; Zhu, Y.; Jagadish, C.; Shen, S. C.; Chen, Z. *Nano Lett.* **2012**, *12*, 3455−3459.
(21) Dousse, A.; Suffczyński, J.; Beveratos, A.; Krebs, O.; Lemaître, A.; Sagnes, I.; Bloch, J.; Voisin, P.; Senellart, P. *Nature* **2010**, *466*, 217−220.
(22) Peter, E.; Senellart, P.; Martrou, D.; Lemaître, A.; Hours, J.; Gérard, J. M.; Bloch, J. *Phys. Rev. Lett.* **2005**, *95*, No. 067401.
(23) Savasta, S.; Saija, R.; Ridolfo, A.; Di Stefano, O.; Denti, P.; Borghese, F. *ACS Nano* **2010**, *4*, 6369−6376.
(24) Murray, C. B.; Norris, D. J.; Bawendi, M. G. *J. Am. Chem. Soc.* **1993**, *115*, 8706−8715.

(25) Tang, Z.; Kotov, N. A.; Giersig, M. *Science* **2002**, *297*, 237−240.
(26) Sung, Y.-M.; Kwak, W.-C.; Kim, T. G. *Cryst. Growth Des.* **2008**, *8*, 1186−1190.
(27) Beaulac, R.; Archer, P. I.; van Rijssel, J.; Meijerink, A.; Gamelin, D. R. *Nano Lett.* **2008**, *8*, 2949−2953.
(28) Beaulac, R.; Schneider, L.; Archer, P. I.; Bacher, G.; Gamelin, D. R. *Science* **2009**, *325*, 973−976.
(29) Bussian, D. A.; Crooker, S. A.; Yin, M.; Brynda, M.; Efros, A. L.; Klimov, V. I. *Nat. Mater.* **2009**, *8*, 35−40.
(30) Qiu, Y.; Chen, W.; Yang, S.; Zhang, B.; Zhang, X. X.; Zhong, Y. C.; Wong, K. S. *Cryst. Growth Des.* **2010**, *10*, 177−183.
(31) White, M. A.; Weaver, A. L.; Beaulac, R.; Gamelin, D. R. *ACS Nano* **2011**, *5*, 4158−4168.
(32) Nann, T.; Skinner, W. M. *ACS Nano* **2011**, *5*, 5291.
(33) Upcher, A.; Ezersky, V.; Berman, A.; Golan, Y. *Cryst. Growth Des.* **2013**, *13*, 2149−2160.
(34) Pacuski, W.; Kruse, C.; Figge, S.; Hommel, D. *Appl. Phys. Lett.* **2009**, *94*, No. 191108.
(35) Tinjod, F.; Gilles, B.; Moehl, S.; Kheng, K.; Mariette, H. *Appl. Phys. Lett.* **2003**, *82*, 4340−4342.
(36) Wojnar, P.; Suffczyński, J.; Kowalik, K.; Golnik, A.; Karczewski, G.; Kossut, J. *Phys. Rev. B* **2007**, *75*, No. 155301.
(37) Maingault, L.; Besombes, L.; Léger, Y.; Bougerol, C.; Mariette, H. *Appl. Phys. Lett.* **2006**, *89*, No. 193109.
(38) Léger, Y.; Besombes, L.; Maingault, L.; Ferrand, D.; Mariette, H. *Phys. Rev. Lett.* **2005**, *95*, No. 047403.
(39) Jakubczyk, T.; Pacuski, W.; Smoleński, T.; Golnik, A.; Florian, M.; Jahnke, F.; Kruse, C.; Hommel, D.; Kossacki, P. *Appl. Phys. Lett.* **2012**, *101*, No. 132105.
(40) Jakubczyk, T.; Pacuski, W.; Smoleński, T.; Golnik, A.; Florian, M.; Jahnke, F.; Kruse, C.; Hommel, D.; Kossacki, P. *J. Appl. Phys.* **2013**, *113*, No. 136504.